

The Fano Effect in Aharonov-Bohm interferometers *

O. Entin-Wohlman^a, A. Aharony^a, Y. Imry^b and Y. Levinson^b

^a*School of Physics and Astronomy, Raymond and Beverly Sackler Faculty of Exact Sciences,
Tel Aviv University, Tel Aviv 69978, Israel*

^b*Department of Condensed Matter Physics, The Weizmann Institute of Science, Rehovot 76100, Israel
(August 21, 2019)*

After briefly reviewing the Fano effect, we explain why it may be relevant to various types of Aharonov-Bohm interferometers. We discuss both closed (electron conserving) and open interferometers, in which one path contains either a simple quantum dot or a decorated quantum dot (with more than one internal state or a parallel path). The possible relevance to some hitherto unexplained experimental features is also discussed.

PACS numbers: 73.63.-b, 03.75.-b, 85.35.Ds

I. INTRODUCTION

In this paper we consider solid-state interferometers, restricted to the mesoscopic scale in order to retain the coherence of the conduction electrons [1]. Here the two-slit geometry is often replaced by narrow waveguides, possibly containing scatterers [2], for the electron paths. An Aharonov-Bohm (AB) [3] flux Φ between the two paths in such interferometers [4,5] yields a conductance $G(\Phi)$ which contains an interference term proportional to $\cos(\phi + \beta)$, where $\phi = 2\pi\Phi/\Phi_0$, and $\Phi_0 = hc/e$ is the single-electron flux quantum. Experiments with a quantum dot (QD) on one of the interfering paths aim to relate β to the dot's intrinsic [6] Friedel [7] transmission phase, α_1 . For closed systems, which conserve the electron current (unitarity), time-reversal symmetry requires via the Onsager relation [8] that $G(\Phi) = G(-\Phi)$, and therefore that $\beta = 0$ or π . Thus, to measure a non-trivial value of β one has to open up the system in order to break unitarity. For open systems, it was recently shown [9] that β depends in general on the details of the broken unitarity. Specific ways of opening the system were discussed, so that the transmission amplitude through the two paths is equal to the sum of the transmission amplitudes through the two individual paths, as in the textbook two-slit geometry [10–12]. In this case, β is equal to the phase difference between these two amplitudes, $\alpha_1 - \alpha_2$, and one gets direct information on α_1 .

The AB h/e oscillations in $G(\Phi)$, first suggested (in spite of strong impurity scattering) in Ref. [4], were subsequently observed on metallic closed systems [5] and in semiconducting samples containing QDs near Coulomb blockade (CB) resonances [13,14]. In these experiments $G(\Phi) = G(-\Phi)$, as required by the Onsager symmetry. Further experiments [14–18] used *open systems*, in which electrons are lost (going to other electron reservoirs) from the transmitted current, to obtain a non-zero phase shift β . Assuming that $\beta = \alpha_2 - \alpha_1$, some of the surprising experimental results were inconsistent with the theoretical expectations for the phase α_1 of the intrinsic transmission through the QD [6,7,19]. Examples include period doubling for the oscillation as function of the gate voltage [13], the phase lapse between consecutive CB resonances [15,16] and the non-universal phase shifts [7,19] at the Kondo resonances [17,18]. These findings have, as yet, not received a universally accepted explanation.

As discussed in Ref. [9], even the unitary (current conserving) interferometer (shown in Fig. 1a) reveals very useful information on the resonances of the QD: although the dependence of G on ϕ is only via $\cos\phi$, so that $\beta = 0$ or $\beta = \pi$, the coefficient of $\cos\phi$ in G changes sign near each resonance, and this could be described as “jumps” of β from zero to π or vice versa. In addition to the vanishing of this coefficient, it turns out that the whole conductance may also vanish (or become very small) at special values of the parameters. For an appropriate choice of parameters, when one may use a perturbative calculation, this also happens close to the resonances. As we discuss below, these zeroes are directly related to a destructive interference between the two paths, in close analogy with the Fano effect [20–23], which concerns destructive interference in the absorption lines between discrete levels and the continuum. In the present paper we elaborate on these phenomena.

*Dedicated to Peter Wölfle on the occasion of his 60th birthday

Having discussed the elementary closed interferometer, we then consider a more complex situation. We introduce a miniature version of the previous closed ring (made of two parallel paths, with a QD on one or on both), as our effective scattering element. We call this combined element the decorated quantum dot (DEQD). We place this DEQD on one path of a larger AB interferometer, as shown in Fig. 1b. (Another example of such a DEQD is a QD with two resonances.) The DEQD, which now replaces the simpler QD of Fig. 1a, captures situations in which one can have internal interference inside the QD. The Fano zeroes of the DEQD have a profound effect on the interference part of the conductance of the whole AB interferometer consisting of the DEQD and the other conducting branch of the AB interferometer. Opening the larger interferometer, so that it obeys the two-slit rules, this procedure allows a measurement of the phase shift associated with the DEQD. The latter is by itself sensitive to the Fano effect. This “hierarchical Fano effect” is the main subject of the present paper. Note that the area subtended between the conducting branch and the DEQD branch is finite and the flux through it is significant, unlike that of the “miniature” conducting branch of the DEQD itself.

In Sec. II we briefly review the original Fano derivation [20], and present an argument for its physical relevance for AB interferometers. We then present calculations on two types of AB interferometers which exhibit the Fano effect and demonstrate the above general arguments. In Sec. III we follow Ref. [4], treating each scattering element via its scattering matrix. A simple tight binding model, based on Ref. [9], is presented in section IV (see fig. 1c). Some technical details of the solution are given in the appendix. The consequences of such models are argued in section V to be rather generic, and results from various other models are cited to support that. The possible relevance to experiments on AB interferometers is then briefly discussed.

II. FANO PHYSICS

In 1961, Fano [20] considered a physical situation which occurs in many systems addressed spectroscopically. In the first part of the calculation, a quantum state, $|\phi\rangle$, with energy E_ϕ^0 , is taken to be coupled via matrix elements $V_{E'}$ to a continuum of states denoted by $|E'\rangle$, forming a resonance in the continuum. In the second part, a transition between another state, $|i\rangle$, (which is not resonant with the continuum) and the resonance is considered, and it is shown that the interference between the contributions of the original continuum states and the resonance will always yield an energy at which the total transition amplitude vanishes. Fano also treated various generalizations which will not be discussed here. In this section we first give a brief review of Fano’s derivation, and then discuss its relevance to interferometers.

A. Fano’s derivation

We start with a quasicontinuum having $N \gg 1$ nondegenerate states, with a very small, roughly uniform, level separation d and a corresponding density of states (DOS) equal to $1/d$. The exact eigenstate with energy \mathcal{E} is written as

$$|\Psi_{\mathcal{E}}\rangle = a_{\mathcal{E}}|\phi\rangle + \sum b_{\mathcal{E},E'}|E'\rangle. \quad (1)$$

The Schrödinger equation for this state becomes

$$\begin{aligned} E_\phi^0 a_{\mathcal{E}} + \sum b_{\mathcal{E},E'} V_{E'}^* &= \mathcal{E} a_{\mathcal{E}}, \\ a_{\mathcal{E}} V_{E'} + b_{\mathcal{E},E'} E' &= \mathcal{E} b_{\mathcal{E},E'}. \end{aligned} \quad (2)$$

For a discrete spectrum of E' , no matter how dense, the well known solution of these equations is found by solving the second equation, $b_{\mathcal{E},E'} = a_{\mathcal{E}} V_{E'} / (\mathcal{E} - E')$, and plugging this value into the first one. The new energies \mathcal{E} are then obtained from the equation

$$\mathcal{E} = E_\phi^0 + \sum |V_{E'}|^2 / (\mathcal{E} - E'). \quad (3)$$

It has already been found by Rayleigh that $N - 1$ of the new energies, \mathcal{E} , straddle the old ones E' , and two states are outside of the original band. Assuming that no localized states occur at finite distances from the band edges, there is a resonance within the band, centered near \mathcal{E}_ϕ (see below). This resonance alters the total DOS everywhere only by relative order $1/N$, and the $b_{\mathcal{E},E'}$ ’s have significant values over a width $(\mathcal{E} - \mathcal{E}_\phi)$ of order $V_{\mathcal{E}_\phi}$. The last term in

Eq. (3) represents the “self consistent” repulsion of the exact energy \mathcal{E} by the band states. For a symmetric $|V_E|$ and a symmetric band, this term vanishes in the middle of the band. A similar level repulsion shifts the peak of the resonance from E_ϕ^0 to \mathcal{E}_ϕ .

We now go to the continuum limit, where $d \rightarrow 0$, $N \rightarrow \infty$ and Nd remains finite, yielding a $O(N)$ density of states $\rho(E) \sim \frac{1}{d}$. In this limit one also has $V_E \rightarrow 0$ but the combination

$$\gamma(E) = |V_E|^2 \rho(E) \quad (4)$$

remains finite. The sums now go into integrals with the DOS, which will basically convert $|V_{E'}|^2$ in the sums into γ in the integrals. The nontrivial mathematical point in solving Eq. (2) in the continuum limit, is in the inversion of $\mathcal{E} - E'$. This is what Fano did extremely carefully. Formally, the solution for $b_{\mathcal{E}, E'}$ from the second equation, can be written as

$$b_{\mathcal{E}, E'} = [\mathcal{P} \frac{1}{\mathcal{E} - E'} + z(\mathcal{E}) \delta(\mathcal{E} - E')] V_{E'} a_{\mathcal{E}}. \quad (5)$$

One is used to writing $z(\mathcal{E}) = i\pi$. However, as pointed out by Fano, for stationary states, one must *determine* $z(\mathcal{E})$ from Eqs. (2). The first of these equations, corresponding to Eq. (3) in the discrete case, becomes then

$$\mathcal{E} = E_\phi^0 + z(\mathcal{E})\gamma + \mathcal{P} \int dE' \gamma(E')/(\mathcal{E} - E') \quad (6)$$

and $z(\mathcal{E})$ is given by

$$z(\mathcal{E}) = \frac{\mathcal{E} - E_\phi^0 - \mathcal{P} \int dE' \gamma(E')/(\mathcal{E} - E')}{\gamma(\mathcal{E})}. \quad (7)$$

The principal part of the integral is analogous to the sum in the discrete case and gives the shift [20] of the resonance, from E_ϕ^0 to the new value \mathcal{E}_ϕ , where $z(\mathcal{E}_\phi) = 0$. The fact that z is real is very significant. Only systems satisfying time-reversal symmetry, in which the Hamiltonian matrix is real and symmetric, are considered, and \mathcal{E} is strictly on the real axis. Moreover, an explicit calculation of the normalization factor, $|a_{\mathcal{E}}|^2$ [20], gives a Lorentzian which is centered at \mathcal{E}_ϕ , with width $\pi\gamma$ (we take γ to be much smaller than the bandwidth, which is usually of the order of Nd). Thus, $z(\mathcal{E})$ changes sign at the actual center of the resonance. These facts provide the mathematical basis for the nontrivial effects found by Fano.

As an example of these effects, Fano considers the absorption from some given initial (non-resonating) state, $|i\rangle$, into the state $|\Psi_{\mathcal{E}}\rangle$. Naively, one expects the usual Lorentzian line shape in the absorption, due to the local DOS, which in turn is the total DOS, weighed for each energy by $|a_{\mathcal{E}}|^2$. This does in fact happen for a transition operator ¹ \hat{T} , that has matrix elements $\langle \phi | \hat{T} | i \rangle$ *only* with the state $|\phi\rangle$. Once matrix elements with the original continuum states also exist, $\langle E' | \hat{T} | i \rangle \neq 0$, interference between the two transition amplitudes from $|i\rangle$ to $|\phi\rangle$ and to $|E'\rangle$ will occur. Substituting Eq. (5) into Eq. (1) and turning the sum into an integral, one has

$$\langle i | \hat{T} | \Psi_{\mathcal{E}} \rangle = a_{\mathcal{E}} (\langle i | \hat{T} | \psi \rangle + \rho(\mathcal{E}) V_{\mathcal{E}} z(\mathcal{E}) \langle i | \hat{T} | \mathcal{E} \rangle), \quad (8)$$

where

$$|\psi\rangle = |\phi\rangle + \mathcal{P} \int dE' \rho(E') \frac{V_{E'} |E'\rangle}{\mathcal{E} - E'} \quad (9)$$

indicates the original state $|\phi\rangle$ modified by the coupling to the continuum. It is important to note the effect of adding the second term in Eq. (8): Since $z(\mathcal{E})$ is real, *with opposite signs on the two sides of the resonance*, and since (for a system satisfying time-reversal symmetry) the matrix elements can also be chosen to be real, *the net transition amplitude will always vanish* at some energy \mathcal{E}_0 which satisfies

¹It might seem to the casual reader that \hat{T} is just the portion of the Hamiltonian, say \mathcal{H}_1 , that causes the transition. In this case the transition rate calculated would have been just the one to lowest order in \mathcal{H}_1 . However, the understanding that \hat{T} is the full transition operator implies that all higher order processes have been summed upon, which converts \mathcal{H}_1 into \hat{T} . In the closed interferometer the difference between using just \mathcal{H}_1 and the full \hat{T} amounts to going from the naive two-path expression for the transmission amplitude [for example, the last brackets of the third equality in Eq. (29)] to its full expression there.

$$z(\mathcal{E}_0) = -\frac{\langle i|\hat{T}|\psi\rangle}{\rho(\mathcal{E}_0)V_{\mathcal{E}_0}\langle i|\hat{T}|\mathcal{E}_0\rangle}. \quad (10)$$

This will not be the case for a complex expression (such as that obtained when a magnetic field is applied) as a function of a single real parameter. It has zeroes on the real axis with zero probability. Eq. (8) also modifies the Lorentzian absorption lineshape. The opposite relative phases of the two terms on the two sides of the resonance turn the Fano absorption lineshape asymmetric around the resonance. Such a Fano lineshape occurs very frequently in the spectroscopy of various atomic, molecular and solid state systems.

B. Fano effect in the closed interferometer

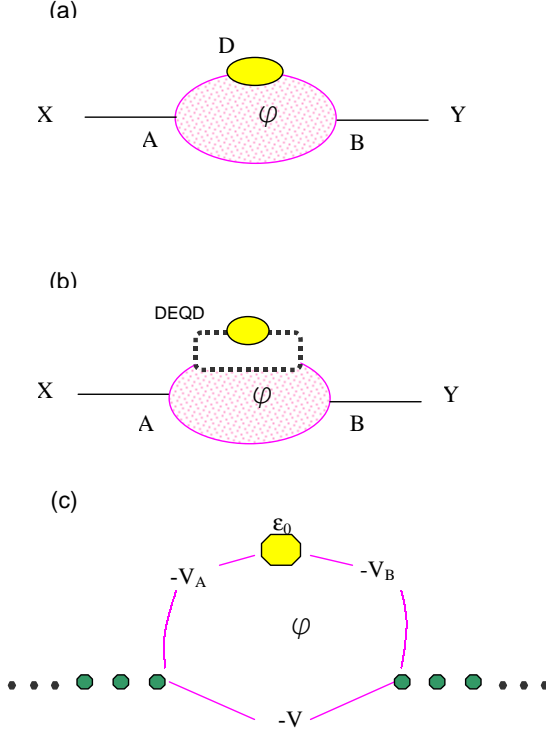


FIG. 1. **(a)** A generic model for a closed AB interferometer having a QD denoted by D on one of its arms. The whole closed interferometer is our DEQD. **(b)** The DEQD in parallel with the conducting arm of the AB interferometer. **(c)** The tight-binding model for the DEQD.

We now give a qualitative explanation why the transition, say, from left to right across the interferometer falls within the Fano discussion. Consider the configuration in Fig. 1a, with a quantum dot D which has one resonance state. Clearly, such transition rates will be governed by the full transition matrix element between the last site on the left (A in the figure) to the first one on the right (B in the figure). As in Sec. IV below, we denote the transfer matrix elements between A and D , D and B and A and B respectively by $-V_A e^{i\phi}$, $-V_B$ and $-V$ (see Fig. 1c). We take $V, V_A, V_B > 0$, ϕ is related to the AB flux, as before, and a gauge putting all the vector potential on the bond of $-V_A$ has been used here. Obviously the results are gauge-invariant. Imagine, just for simplicity, that $|V|, |V_A| \ll |V_B|$, so that the dot D is mainly coupled to the right lead and all the couplings of the left lead are weak perturbations. We first solve exactly the problem of the dot coupled to the right lead, getting the usual resonance state of the dot. Now, we calculate the transition rate from a given state $|i\rangle$ on the left lead to the exact states of the dot-right lead system. Each of the latter is an exact linear combination, as in Eq. (1), of the dot and the right-lead states. The matrix elements between A and the former is $-V_A e^{i\phi}$, and with the latter, it is $-V$. These two correspond to $\langle \phi|\hat{T}|i\rangle$ and $\langle E'|\hat{T}|i\rangle$ respectively. This establishes a full one-to-one correspondence between the Fano problem and the AB interferometer under discussion. As explained above, Fano requires *real* transition amplitudes. Therefore, the Fano effect will only be observed for $\phi = 0$ or $\phi = \pi$. In these cases, the transition probability at some energy (which is

proportional to the transmission coefficient at the same energy), *must* vanish on one side of the resonance. $\mathcal{E}_0 - \mathcal{E}_\phi$ is found to have opposite signs at $\phi = 0$ and $\phi = \pi$.

The above argument appears to have been based on the lowest order golden rule, using only the square of the transition matrix element. As we show below, the same effect appears in the exact solution of this problem, where one sums over all the reflections within the ring [9,4]. This amounts to using, as in the original Fano paper, the full transition operator \hat{T} instead of the perturbation Hamiltonian \mathcal{H}_1 . These exact results show that increasing $|V|$ and $|V_A|$ can only move the zero continuously as function of energy, but a zero will always exist (unless interfered by other bands).

C. Decorated QD in an AB interferometer

Consider next the geometry in Fig. 1b. Here we replace the QD by a small ring, which is itself similar to the whole ring of Fig. 1a. We call this small ring a “decorated QD” (DEQD). The DEQD is now placed on one path of the AB interferometer. The additional path within the DEQD is aimed to allow internal interference, which usually exists due to competing “paths” through the QD. Assuming that the area of the DEQD ring is much smaller than that of the full interferometer, we can neglect the flux through the DEQD. The above Fano argument then implies that the transmission amplitude of the DEQD branch of the AB interferometer, t_{DEQD} , must vanish as function of energy in the vicinity of each resonance.

We now assume that the interferometer is *open*, and that it obeys the necessary conditions for the two-slit equation to hold [9],

$$T_{tot} = |t_{DEQD}e^{i\phi} + t_{par}|^2, \quad (11)$$

where t_{par} is the transmission amplitudes of the large parallel branch of the whole interferometer (see Fig. 1b). We see that the two-path interference part of the AB conductance,

$$T_{int} = 2\mathcal{R}(t_{DEQD}t_{par}^*e^{i\phi}), \quad (12)$$

vanishes and changes sign at the energies of the DEQD Fano zeroes. Thus the transmission phase of the DEQD, as measured by the phase of the AB oscillations, can be said to jump by π at these points [21].

Finally, we reemphasize the importance of going in the golden-rule type calculation for the closed DEQD, from a sum of lowest-order transition amplitudes to one including all the multiple reflections [4]. The universal validity of the Fano zeroes is guaranteed as long as time-reversal symmetry assures that all quantities in the calculation can be chosen real. Interestingly, in this case, gauge invariance assures that one *may* use other choices. This is why deliberately not choosing real parameters was not crucial in the calculation reported below.

III. RESULTS ON A SIMPLE CLOSED INTERFEROMETER

A. The DEQD

In this chapter we consider the model of Ref. [4]. The transmission of a closed ring containing two parallel resistors was calculated exactly. The Landauer formulation with single-channel conductors was used to relate the transmission coefficient to the conductance and the resistors were modelled by elastic scatterers described by 2×2 scattering matrices. Thus, the geometry of the system was similar to that of Fig. 1a, except that two general scatterers are placed each on one of the arms. The transmission amplitudes from the left and from the right respectively are: t_i and t'_i , $i = 1, 2$, and $r_i, (r'_i)$, $i = 1, 2$ are the reflection amplitudes on the left (right) of the scatterer. Notice that time-reversal and current conservation requirements, which imply $t_i = t'_i$ and $-t_i/t_i^* = r_i/r_i^*$ (the asterisk denotes complex conjugation), are also satisfied when the geometrical phases of each path are absorbed in t_i , etc. When an AB magnetic flux Φ is applied through the center of the ring, the transmission and reflection amplitudes pick up the phases $t_1 \rightarrow t_1 e^{i\phi}$, $t'_1 \rightarrow t'_1 e^{-i\phi}$. The three-terminal junctions at the two connections of the ring to the wires were described by a 3×3 unitary (chosen real) scattering matrix [24],

$$S = \begin{pmatrix} 0 & -1/\sqrt{2} & -1/\sqrt{2} \\ -1/\sqrt{2} & 1/2 & -1/2 \\ -1/\sqrt{2} & -1/2 & 1/2 \end{pmatrix}, \quad (13)$$

where the diagonal elements, S_{ii} ($i = 1, 2, 3$) denote the reflection amplitude of the i^{th} channel, and the off-diagonal elements S_{ij} ($i \neq j$) are the transmission amplitudes from channel j to channel i . Channel 1 of the left-hand side junction is chosen to be that of the incoming amplitude (unity) whereas channel 1 of the right hand side junction is that of the outgoing amplitude (F). For this splitter, no reflection occurs in channel 1 and there is symmetry between channels 2 and 3. The results are not expected to depend qualitatively on the choice of the junction's scattering matrix, except for the trivial effect that these junctions are themselves scatterers and add to the total resistance of the device.

From the wave equation for the scattering solution for this model, it was found in Ref. [4] that the total transmission amplitude, F , of the ring is given by

$$F = 2 \frac{t_1 t_2 (t'_1 + t'_2) + t_1 (r_2 - 1)(1 - r'_2) + t_2 (r_1 - 1)(1 - r'_1)}{(t_1 + t_2)(t'_1 + t'_2) - (2 - r_1 - r_2)(2 - r'_1 - r'_2)}. \quad (14)$$

The scatterers ($i = 1, 2$) on the two arms are arbitrary elastic ones. We chose Breit-Wigner forms for them:

$$t_i = t'_i = \frac{i\Gamma_i}{i\Gamma_i - (E - E_i)}, \quad (15)$$

$$r_i = r'_i = \frac{E - E_i}{i\Gamma_i - (E - E_i)}, \quad (16)$$

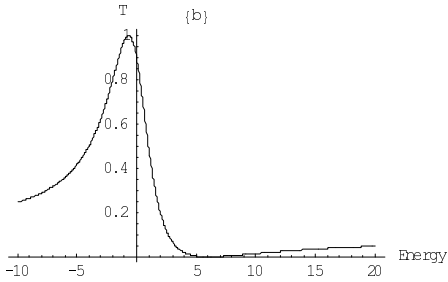
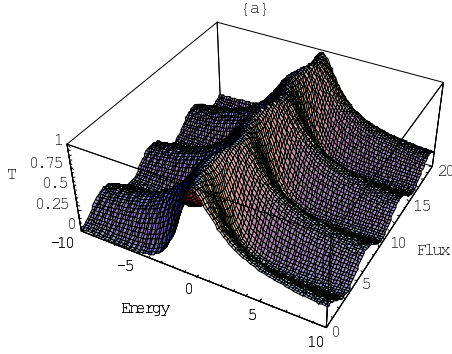


FIG. 2. **(a)** Transmission as function of $E - E_1$ or “gate voltage” and ϕ for the closed interferometer of Ref. [4]. Parameters were such that $\Gamma_1 = 4$, $E_1 = 0$, $\Gamma_2 = 2$, $E - E_2 = 3$ (i.e. an energy-independent transmission on the nonresonant branch). Note the Fano zero at Zero flux and the phase change of π across the resonance. That change happens via the vanishing of the first Fourier component at a point very close to the resonance. **(b)** Transmission as function of $E - E_1$ for $\phi = \pi$, demonstrating a Fano zero. Note its position with respect to the one in Fig. 3a.

For scatterer no. 1 we took a resonance at $E_1 = 0$. The resonance of scatterer 2 was taken further away, so that it can be regarded as approximately non-resonant around the resonance of 1. Results for $T = |F|^2$ as function of energy and flux are depicted in Fig. 2a. The \hbar/e -periodic (period of 2π in ϕ) AB oscillation is clearly seen. This oscillation is even in ϕ , as it should. We display only the $\phi \geq 0$ part, in order to show clearly the Fano-type zero at $\phi = 0$. In addition, one may also observe how the first harmonic (period 2π) of the oscillation vanishes near the resonance, i.e. the sign of that Fourier component reverses there. This simply means that (except for higher harmonics) the behavior around $\phi = 0$ changes from a maximum to a minimum of $|F|^2$. This is how the phase change of π around a resonance manifests itself for this interferometer which satisfies unitarity and the Onsager relationships. For completeness, we display in Fig. 2b the transmission as function of energy at a flux of π , which also shows the Fano zero, as expected. This zero occurs for a positive energy, while the same model (see Fig. 3a later) produces a Fano zero for a negative energy at vanishing flux. This opposite behavior for the two special values of the flux is consistent with ref. [20].

B. The open two-path interferometer with a DEQD on one of its arms

As indicated in the introduction, we now embed the DEQD as our effective scattering element on one of the arms of a large *open* AB interferometer (see Fig. 1b) assumed to be designed so that its transmission is obtained from just adding two paths. We have now simply added the transmission amplitude, t_{DEQD} as obtained from the above results, to that of a far-from-resonance and energy-independent scatterer on the other arm. (The latter models a conducting path which has an energy-independent transmission amplitude given by t_{par}). Now, we plotted the dimensionless conductance of the whole interferometer as a function of energy and flux in Fig. 3b.

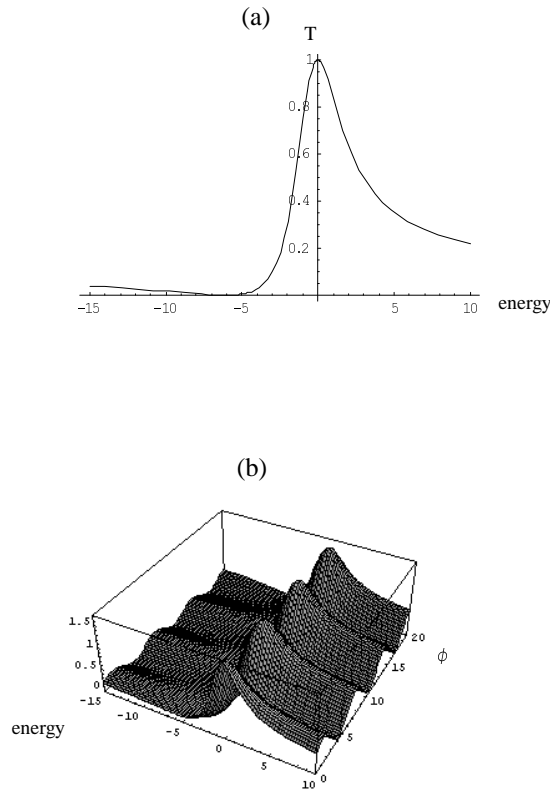


FIG. 3. **(a)** Transmission as a function of “gate voltage” for a DEQD consisting of a QD with a single level at 0 with width of 4, in dimensionless units, in parallel with a nonresonant branch with $t = 2i/(2i - 3)$; $r = 3/(2i - 3)$, (the same as that used in fig. 2a). Note the Fano-type zero at about -5 . **(b)** Transmission as a function of “gate voltage” and flux for the same DEQD embedded in a two-path interferometer with a transmitter of $t_{par} = .3$, mimicking experimental data on a two-path AB interferometer. Note that the phase of the AB oscillation is changing around the peak but it is coming back and it is the same far on the two sides of the peak. This is due to the Fano-type zero and may offer an explanation for the phase lapse of Ref. [16].

We point out that *unlike what happened in the closed “miniature” interferometer constituting the DEQD in Fig. 2a*, the phase of the AB oscillation is changing around the peak but it is “coming back” and becomes the same far on its two sides. Therefore, the phase increase of π around the resonance is “rewound” by the zero in the transmission of the DEQD. This rewinding happens sharply as a function of energy, when the flux-dependence vanishes and changes sign. Thus, the Fano zero in the DEQD produces very interesting effects in the open AB interferometer.

IV. SIMPLE TIGHT-BINDING MODELS

A. A triangular interferometer

In this section we calculate the scattering matrix through a triangle, containing an Aharonov-Bohm flux, see Fig. 1c [9]. The leads are described by a tight-binding model, with hopping amplitudes $-J$, and zero on-site energies, such that the energy of the scattered electron is

$$\epsilon_q = -2J \cos qa. \quad (17)$$

The leads are connected to the triangle at its sites A (left) and B (right). The third site D is the “quantum dot” (QD). The direct hopping amplitude between A and B is denoted $-V$, and is real. The hopping amplitude from A to D is denoted $-V_A e^{i\phi_A} \equiv -\bar{V}_A$, and the hopping amplitude from D to B is denoted $-V_B e^{i\phi_B} \equiv -\bar{V}_B$. The total Aharonov-Bohm flux is

$$\Phi = \frac{e}{\hbar c}(\phi_A + \phi_B) = \frac{e}{\hbar c}\phi. \quad (18)$$

The Hamiltonian of the system is

$$\mathcal{H} = \mathcal{H}_0 + \mathcal{H}_1, \quad (19)$$

where \mathcal{H}_0 is the Hamiltonian of the ordered chain (with V replaced by J), and the isolated QD (with site energy ϵ_0), and

$$\begin{aligned} \mathcal{H}_1(\ell, m) = & -\bar{V}_A \delta_{\ell A} \delta_{m D} - (\bar{V}_A)^* \delta_{\ell D} \delta_{m A} \\ & - \bar{V}_B \delta_{\ell D} \delta_{m B} - (\bar{V}_B)^* \delta_{\ell B} \delta_{m D} \\ & - (V - J)(\delta_{\ell A} \delta_{m B} + \delta_{\ell B} \delta_{m A}). \end{aligned} \quad (20)$$

The scattering solution is denoted $\Psi(n)$. It is given by

$$\Psi(n) = \Psi_0(n) + \sum_{\ell m} G(n, \ell) \mathcal{H}_1(\ell, m) \Psi_0(m), \quad (21)$$

where Ψ_0 is the incoming wave, so that

$$\begin{aligned} \Psi_0(D) &= 0, \\ \Psi_0(n) &\simeq e^{\pm i q n a}, \end{aligned} \quad (22)$$

the (\pm) represents a wave incident from the left or from the right).

The Green function is calculated from the equation

$$G(n, n') = G_0(n, n') + \sum_{\ell m} G(n, \ell) \mathcal{H}_1(\ell, m) G_0(m, n'), \quad (23)$$

where G_0 is the Green function of \mathcal{H}_0 , so that

$$\begin{aligned} G_0(D, A) &= G_0(A, D) = G_0(D, B) = G_0(B, D) = 0, \\ G_0(A, A) &= G_0(B, B) \equiv g = \frac{1}{2iJ \sin qa}, \\ G_0(A, B) &= G_0(B, A) = g e^{iqa}. \end{aligned} \quad (24)$$

The matrix elements of the Green function are calculated in the appendix. We next express the scattering matrix in terms of $G(D, D)$.

B. Calculation of the scattering matrix

For the sake of concreteness, we assume that the origin is at the mid-point between the sites A and B . Thus

$$\Psi_0 = e^{\pm iqa(n-1/2)}, \quad (25)$$

so that for the wave incident from the left

$$\Psi_0(A) = e^{-iqa/2}, \quad \Psi_0(B) = e^{iqa/2}, \quad \Psi(A) = e^{-iqa/2} + re^{iqa/2}, \quad \Psi(B) = te^{iqa/2}, \quad (26)$$

and for the wave incident from the right

$$\Psi_0(A) = e^{iqa/2}, \quad \Psi_0(B) = e^{-iqa/2}, \quad \Psi(A) = t'e^{iqa/2}, \quad \Psi(B) = e^{-iqa/2} + r'e^{iqa/2}. \quad (27)$$

From the general equations for the scattered wave,

$$\begin{aligned} \Psi(A) &= \Psi_0(A) - (\bar{V}_A)^* G(A, D) \Psi_0(A) - \bar{V}_B G(A, D) \Psi_0(B) \\ &\quad - (V - J) G(A, A) \Psi_0(B) - (V - J) G(A, B) \Psi_0(A), \\ \Psi(B) &= \Psi_0(B) - (\bar{V}_A)^* G(B, D) \Psi_0(A) - \bar{V}_B G(B, D) \Psi_0(B) \\ &\quad - (V - J) G(B, A) \Psi_0(B) - (V - J) G(B, B) \Psi_0(A). \end{aligned} \quad (28)$$

From all the above, we obtain

$$\begin{aligned} 1 + re^{iqa} &= 2iJ \sin qa \frac{G(D, D)}{\frac{V^2}{J} e^{iqa} - J e^{-iqa}} \times \left(\epsilon_q - \epsilon_0 + \frac{V_B^2}{J} e^{iqa} \right), \\ 1 + e^{iqa} r' &= 2iJ \sin qa \frac{G(D, D)}{\frac{V^2}{J} e^{iqa} - J e^{-iqa}} \times \left(\epsilon_q - \epsilon_0 + \frac{V_A^2}{J} e^{iqa} \right), \\ t &= 2iJ \sin qa \frac{G(D, D)}{\frac{V^2}{J} e^{iqa} - J e^{-iqa}} \times \left(\frac{V}{J} (\epsilon_q - \epsilon_0) - \frac{(\bar{V}_A \bar{V}_B)^*}{J} \right), \\ t' &= 2iJ \sin qa \frac{G(D, D)}{\frac{V^2}{J} e^{iqa} - J e^{-iqa}} \times \left(\frac{V}{J} (\epsilon_q - \epsilon_0) - \frac{\bar{V}_A \bar{V}_B}{J} \right). \end{aligned} \quad (29)$$

It is interesting to note that the information on the QD enters the scattering matrix via the Green function on the dot, $G(D, D)$. As shown by Ng and Lee [6], this remains true also when one includes electron-electron interactions on the QD. The important fact is that the interference part, reflected by the terms in brackets in t and t' in Eq. (29), has real coefficients except for the AB phase factor $e^{i\phi}$.

We are now ready to calculate the transmission. From Eq. (A3), we write

$$\begin{aligned} G^{-1}(D, D) &= \epsilon_q - \epsilon_0 + \frac{\frac{V_A^2 + V_B^2}{J} e^{iqa} + 2 \frac{V}{J} \frac{V_A V_B}{J} \cos \phi e^{2iqa}}{1 - \left(\frac{V}{J} \right)^2 e^{2iqa}} \\ &\equiv \mathcal{A} + i\mathcal{B}, \end{aligned} \quad (30)$$

with

$$\begin{aligned} \mathcal{A} &= \epsilon_q - \epsilon_0 \\ &\quad + \frac{\frac{V_A^2 + V_B^2}{J} \cos qa \left(1 - \left(\frac{V}{J} \right)^2 \right) + 2 \frac{V}{J} \frac{V_A V_B}{J} \cos \phi \left(\cos 2qa - \left(\frac{V}{J} \right)^2 \right)}{1 + \left(\frac{V}{J} \right)^4 - 2 \left(\frac{V}{J} \right)^2 \cos 2qa}, \\ \mathcal{B} &= \frac{\frac{V_A^2 + V_B^2}{J} \sin qa \left(1 + \left(\frac{V}{J} \right)^2 \right) + 2 \frac{V}{J} \frac{V_A V_B}{J} \cos \phi \sin 2qa}{1 + \left(\frac{V}{J} \right)^4 - 2 \left(\frac{V}{J} \right)^2 \cos 2qa}. \end{aligned} \quad (31)$$

We then define the ‘‘Friedel phase’’ of the QD [7,6], ϕ_D , such that

$$\cot \phi_D = -\frac{\mathcal{A}}{\mathcal{B}}, \quad (\sin^2 \phi_D = \frac{\mathcal{B}^2}{\mathcal{A}^2 + \mathcal{B}^2}, \quad \cos^2 \phi_D = \frac{\mathcal{A}^2}{\mathcal{A}^2 + \mathcal{B}^2}), \quad (32)$$

which gives

$$G(D, D) = -\frac{\sin \phi_D}{\mathcal{B}} e^{i\phi_D}. \quad (33)$$

The phase ϕ_D is usually referred to as the “intrinsic transmission phase” of the dot. When the dot is placed on path 1 of the AB interferometer, ϕ_D is equal to the phase α_1 mentioned in our introduction. The transmission of the structure can now be written in the form

$$T = |t|^2 = \frac{4 \sin^2 qa}{1 + \left(\frac{V}{J}\right)^4 - 2\left(\frac{V}{J}\right)^2 \cos 2qa} \times \frac{\sin^2 \phi_D}{\mathcal{B}^2} \times \left\{ \left(\frac{V}{J}\right)^2 (\epsilon_q - \epsilon_0)^2 + \left(\frac{V_A V_B}{J}\right)^2 - 2\frac{V}{J} \frac{V_A V_B}{J} (\epsilon_q - \epsilon_0) \cos \phi \right\}. \quad (34)$$

Let us now manipulate the term in the curly brackets. From the equations for \mathcal{A} and \mathcal{B} we can write

$$\begin{aligned} \epsilon_q - \epsilon_0 &= \mathcal{A} - \frac{1 - \left(\frac{V}{J}\right)^2}{1 + \left(\frac{V}{J}\right)^2} \cot qa \mathcal{B} + 2\frac{V}{J} \frac{V_A V_B}{J} \cos \phi, \\ \frac{V_A^2 + V_B^2}{J} &= \frac{1 + \left(\frac{V}{J}\right)^4 - 2\left(\frac{V}{J}\right)^2 \cos 2qa}{1 + \left(\frac{V}{J}\right)^2} \frac{\mathcal{B}}{\sin qa} - \frac{4\frac{V}{J}}{1 + \left(\frac{V}{J}\right)^2} \frac{V_A V_B}{J} \cos \phi \cos qa. \end{aligned} \quad (35)$$

Hence the term in the curly brackets becomes

$$\begin{aligned} \left\{ \right\} &= \left(\frac{V_A V_B}{J}\right)^2 \sin^2 \phi + \left[\frac{V}{J} (\epsilon_q - \epsilon_0) - \frac{V_A V_B}{J} \cos \phi \right]^2 \\ &= \left(\frac{V_A V_B}{J}\right)^2 \sin^2 \phi + \left[\frac{V}{J} \mathcal{A} - \frac{1 - \left(\frac{V}{J}\right)^2}{1 + \left(\frac{V}{J}\right)^2} \left(\frac{V}{J} \mathcal{B} \cot qa + \frac{V_A V_B}{J} \cos \phi \right) \right]^2. \end{aligned} \quad (36)$$

Putting all this together, we obtain

$$\begin{aligned} T &= \frac{4 \sin^2 qa}{1 + \left(\frac{V}{J}\right)^4 - 2\left(\frac{V}{J}\right)^2 \cos 2qa} \left\{ \left(\frac{V_A V_B \sin \phi_D \sin \phi}{J \mathcal{B}} \right)^2 \right. \\ &\quad \left. + \left(\frac{V}{J} \left(\cos \phi_D + \frac{1 - \left(\frac{V}{J}\right)^2}{1 + \left(\frac{V}{J}\right)^2} \cot qa \sin \phi_D \right) + \frac{1 - \left(\frac{V}{J}\right)^2}{1 + \left(\frac{V}{J}\right)^2} \frac{V_A V_B}{J \mathcal{B}} \cos \phi \sin \phi_D \right)^2 \right\}. \end{aligned} \quad (37)$$

C. Fano effect

From Eq. (29), the transmission amplitude contains three factors:

$$t = CG(D, D)[V(\epsilon_q - \epsilon_0) - V_A V_B e^{-i\phi}], \quad (38)$$

where $C = 2iJ \sin qa / (V^2 e^{iqa} - J^2 e^{-iqa})$ does not depend on ϕ and does not exhibit any interesting features near the resonance. The interference is mainly reflected by the square brackets. Since all the coefficients inside these brackets

are real, the absolute value of these brackets depends only on $\cos \phi$, as required by Onsager. $\cos \phi$ also appears in $G(D, D)$, see Eq. (30). Expanding $|G(D, D)|^2$ in a Fourier series in ϕ , one has

$$|G(D, D)|^2 = g_0 + g_1 \cos \phi + g_2 \cos 2\phi + \dots \quad (39)$$

Thus, the coefficient of $\cos \phi$ in $T = |t|^2$ is proportional to

$$[V^2(\epsilon_q - \epsilon_0)^2 + V_A^2 V_B^2] g_1 - 2V V_A V_B (\epsilon_q - \epsilon_0) g_0. \quad (40)$$

For small $V_A V_B$ and/or $\frac{g_1}{g_0}$, this vanishes at some energy ϵ_q close to the original resonance ϵ_0 . As explained above, such vanishing can be interpreted as a “jump” of the phase shift β by π .

For a flux $\phi = n\pi$ with integer n , the square brackets in Eq. (38) are real, and the whole square brackets vanish at $(\epsilon_q - \epsilon_0) = (-1)^n V_A V_B / V$. This is exactly the Fano effect and it arises from the exact solution, without the lowest order golden rule approximation. For small $V_A V_B$ this vanishing of T (and thus of the conductance) is also close to the original resonance. If ϕ is close to such integer values, there will be a dip in G as function of ϵ_q . We expect similar dips in G and “phase slips” by π near every resonance.

D. Special Cases

We now consider the following special cases:

1. $V = 0$. This is the Ng-Lee model [6]. We find

$$\mathcal{B} = \frac{V_A^2 + V_B^2}{J} \sin qa, \quad (41)$$

and hence the transmission is

$$T = \sin^2 \phi_D \left(\frac{2V_A V_B}{V_A^2 + V_B^2} \right)^2, \quad (42)$$

which becomes just $\sin^2 \phi_D$ when $V_A = V_B$.

2. $V = J$. In this case

$$\mathcal{B} = \frac{\frac{V_A^2 + V_B^2}{J} + 2\frac{V_A V_B}{J} \cos \phi \cos qa}{2 \sin qa}, \quad (43)$$

and the transmission is

$$T = \cos^2 \phi_D + \left(\frac{V_A V_B \sin \phi}{J \mathcal{B}} \right)^2 \sin^2 \phi_D. \quad (44)$$

We note that the model of Kang *et al.* [25] corresponds to putting either V_A or V_B equal to zero. Then the transmission is just $\cos^2 \phi_D$, and the transmission phase shift at resonance becomes π . The result (44) can be put in the form

$$T = \cos^2 \phi_D + \sin^2 \phi_D \left(\frac{\frac{2V_A V_B}{J} (\cos^2 \frac{\phi - qa}{2} - \cos^2 \frac{\phi + qa}{2})}{\left(\frac{V_A - V_B}{J} \right)^2 + 2\frac{V_A V_B}{J} (\cos^2 \frac{\phi + qa}{2} + \cos^2 \frac{\phi - qa}{2})} \right)^2. \quad (45)$$

The maximal transmission is achieved for $V_A = V_B$, and is a combination of $\cos \phi_D$ and $\sin \phi_D$ terms. Note especially the way the magnetic field phase, ϕ , appears here. The full expression is of course even in ϕ .

3. $V \gg J$. In this case

$$\mathcal{B} \simeq \left(\frac{J}{V}\right)^2 \frac{V_A^2 + V_B^2}{J} \sin qa, \quad (46)$$

and to leading order

$$T \rightarrow \sin^2 \phi_D \left(\frac{2V_A V_B}{V_A^2 + V_B^2} \right)^2, \quad (47)$$

namely, the Ng-Lee result. It is very interesting that the limit of a strong coupling in the tight-binding model is similar to a vanishing coupling.

4. The symmetric case in which $V_A = V_B = V$. This assumption does not simplify considerably the expression for the transmission. However, it is interesting to note that V will drop out from the result for T (except that it enters back in the definition of ϕ_D).

E. A QD with two resonances

One way to decorate the dot is to allow more than one state on it. The effects of two paths in the DEQD is thus replaced by having two levels on the bare dot, ϵ_0 and ϵ_1 . The couplings of the new level to the “forks” A and B are then modeled by the additional tight-binding terms,

$$\Delta\mathcal{H}_1 = -V_1 e^{i\phi_1} \delta_{\ell A} \delta_{mD} - V_2 e^{i\phi_2} \delta_{\ell D} \delta_{mB} + \text{h.c.}, \quad (48)$$

where we assume the same total flux, $\phi = \phi_1 + \phi_2$. The paths going through this level simulate the small parallel conducting branch in the DEQD.

It is straightforward to repeat the calculation of the scattering matrix. The result is

$$\begin{aligned} t' &= 2iJ \sin qa e^{iqa} \left[-V + e^{i\phi} \left(\frac{V_A V_B}{\epsilon_q - \epsilon_0} + \frac{V_1 V_2}{\epsilon_q - \epsilon_1} \right) \right] \mathcal{D}^{-1}, \\ 1 + r' e^{iqa} &= -2iJ \sin qa e^{iqa} \left[1 + e^{iqa} \left(\frac{V_A^2}{\epsilon_q - \epsilon_0} + \frac{V_1^2}{\epsilon_q - \epsilon_1} \right) \right] \mathcal{D}^{-1}, \end{aligned} \quad (49)$$

with analogous results for t and r . Here, \mathcal{D} is related to the 2×2 Green matrix on the two states of the QD. It depends on ϕ only via $\cos \phi$.

It is interesting to note that the interference part, contained in the square brackets in t' , contains the factor

$$\mathcal{X} = \frac{V_A V_B}{\epsilon_q - \epsilon_0} + \frac{V_1 V_2}{\epsilon_q - \epsilon_1}, \quad (50)$$

which plays the role of

$$\frac{V_A V_B}{\epsilon_q - \epsilon_0} \quad (51)$$

in the previous results. The Fano effect, i. e. the vanishing of t' , will now occur when

$$\mathcal{X}(\epsilon_q) = V. \quad (52)$$

If $V_A V_B / (V_1 V_2)$ were positive, then this equation always has two solutions, one being between the original resonance and the other being below or above both. However, usually the two resonances on the QD correspond to states of opposite parity. In that case, the ratio is negative, and the equation may have no real solutions, or both solutions between the original resonances (or on one side of both), or one solution on each side of both resonances. This argument can easily be extended to more resonances: \mathcal{X} simply becomes a sum of terms like $V_{L,j} V_{R,j} / (\epsilon_q - \epsilon_j)$, and the Fano zeroes either appear between every pair of original resonances, or are paired alternately between them. In any case, in most of the cases one will have a Fano zero associated with each original resonance.

In addition to the Fano point, each resonance is usually also associated with a nearby point at which the phase β jumps by π . This happens when ϵ_q obeys the equation

$$(V^2 + \mathcal{X}^2) d_1 - 2V \mathcal{X} d_0 = 0, \quad (53)$$

where we used the Fourier expansion $|\mathcal{D}|^{-2} = d_0 + d_2 \cos \phi + \dots$

V. THE GENERALITY OF THE MODEL AND ITS PHYSICAL CONSEQUENCES

In Sec. II we stated that the Fano zeroes are rather universal for AB interferometers. In addition to our considerations there, we found these zeroes in both the scattering model of Ref. [4], treated in Sec. III, and in the tight-binding model of Ref. [9], generalized in Sec. IV. They also appear for two coupled resonances, many coupled resonances and with generic parallel conducting branches. These results are not peculiar to specific features, such as the “fork” 3×3 matrix used in Ref. [4]. We point out that such zeroes actually appeared also in Ref. [26] which used a different class of “fork” matrices. More interestingly, the conditions for the effect are much more general than having a QD on one of the branches. We find that Fano zeroes appear also by analyzing the tight-binding model of Ref. [27] as well as in the model of Ref. [28], with “QD’s” on *both* branches. Fano-type zeroes appear in the problem of two levels coupled to reservoirs [20] and such a zero also shows up in the level statistics (see the inset to Fig. 1 of Ref. [29]). Thus, it is unlikely that the Fano effect will not play a role in the physics of AB interferometers and coupled QD’s.

Fano physics may well be relevant for the understanding of a number of experimental anomalies found in interferometers containing quantum dots. The results in section IV show how the transmission phase at resonance (which should also be valid for a Kondo resonance) changes from $\pi/2$ in the simple QD to π for a DEQD with $V = J$ (see also Refs. [25,22,23]). This phase shift will be measured in an open AB interferometer which obeys the two-slit conditions. A number of specific mechanisms using variations of the Fano model have in fact also been advanced [21] as to the relevance of the Fano effect to the “phase lapse” discovered experimentally [14–18] in AB interferometers containing QD’s. Related particular mechanisms are based on the superposition of many resonances [30]. (This in fact can be taken as a particular realization of the parallel conducting channel model). In the simplest model of two adjacent Breit-Wigner resonances, one finds that if signs are right, an approximate zero in the transmission must occur in-between them. However, within the Breit-Wigner approximation to the resonances, the zero is off the real energy axis by about the width of these resonances (taken, for simplicity to have comparable widths). What the Fano considerations tell us, however, is that the zero is exactly on the real axis and therefore the “phase lapse” should be sharp. The Fano-type considerations therefore augment these models in a significant fashion. Here we tried to treat all these Fano-related considerations in a simple and unified fashion. More work is needed, however, to examine whether the Fano effect may really offer a valid explanation for the experimentally observed phase lapses.

APPENDIX A: CALCULATION OF THE GREEN FUNCTION

Our aim here is to calculate the (D, D) matrix element of the Green function. We have

$$\begin{aligned}
 G(D, D) &= G_0(D, D) - \bar{V}_A G(D, A) G_0(D, D) - (\bar{V}_B)^* G(D, B) G_0(D, D), \\
 G(D, A) &= -(\bar{V}_A)^* G(D, D) G_0(A, A) - \bar{V}_B G(D, D) G_0(B, A) \\
 &\quad - (V - J) [G(D, A) G_0(B, A) + G(D, B) G_0(A, A)], \\
 G(D, B) &= -(\bar{V}_A)^* G(D, D) G_0(A, B) - \bar{V}_B G(D, D) G_0(B, B) \\
 &\quad - (V - J) [G(D, A) G_0(B, B) + G(D, B) G_0(A, B)].
 \end{aligned} \tag{A1}$$

Using the results

$$\begin{aligned}
 G_0(A, A) &= G_0(B, B) \equiv g = \frac{1}{2iJ \sin qa}, \\
 G_0(A, B) &= G_0(B, A) = g e^{iqa},
 \end{aligned} \tag{A2}$$

(where it is assumed that A and B are separated by the same lattice constant as on the leads), we find

$$\begin{aligned}
 G(D, D) &\equiv [\epsilon_q - \epsilon_0 - \Sigma(D, D)]^{-1} \\
 \Sigma(D, D) &= \frac{V_A^2 + V_B^2 + 2\frac{V}{J} V_A V_B e^{iqa} \cos \phi}{\frac{V^2}{J} e^{iqa} - J e^{-iqa}},
 \end{aligned} \tag{A3}$$

and

$$\begin{aligned}
G(D, A) &= -\frac{G(D, D)}{\frac{V^2}{J}e^{iqa} - Je^{-iqa}} \left((\bar{V}_A)^* + \frac{V}{J}\bar{V}_B e^{iqa} \right), \\
G(D, B) &= -\frac{G(D, D)}{\frac{V^2}{J}e^{iqa} - Je^{-iqa}} \left(\bar{V}_B + \frac{V}{J}(\bar{V}_A)^* e^{iqa} \right).
\end{aligned} \tag{A4}$$

The scattering solution requires the matrix elements

$$G(A, D), \quad G(A, A), \quad G(A, B), \quad G(B, D), \quad G(B, A), \quad G(B, B). \tag{A5}$$

We have the equations

$$\begin{aligned}
G(A, D) &= -\bar{V}_A G(A, A) G_0(D, D) - (\bar{V}_B)^* G(A, B) G_0(D, D), \\
G(B, D) &= -\bar{V}_A G(B, A) G_0(D, D) - (\bar{V}_B)^* G(B, B) G_0(D, D), \\
G(A, A) &= g - (\bar{V}_A)^* G(A, D) g - \bar{V}_B G(A, D) g e^{iqa} - (V - J) g \left(G(A, A) e^{iqa} + G(A, B) \right), \\
G(A, B) &= g e^{iqa} - (\bar{V}_A)^* G(A, D) g e^{iqa} - \bar{V}_B G(A, D) g - (V - J) g \left(G(A, A) + G(A, B) e^{iqa} \right), \\
G(B, A) &= g e^{iqa} - (\bar{V}_A)^* G(B, D) g - \bar{V}_B G(B, D) g e^{iqa} - (V - J) g \left(G(B, A) e^{iqa} + G(B, B) \right), \\
G(B, B) &= g - (\bar{V}_A)^* G(B, D) g e^{iqa} - \bar{V}_B G(B, D) g - (V - J) g \left(G(B, A) + G(B, B) e^{iqa} \right).
\end{aligned} \tag{A6}$$

The third and fourth equations here give

$$\begin{aligned}
G(A, A) \frac{V}{J} e^{iqa} - G(A, B) &= -G(A, D) \frac{\bar{V}_B}{J} e^{iqa}, \\
G(A, B) \frac{V}{J} e^{iqa} - G(A, A) &= \frac{1}{J} e^{iqa} - \frac{(\bar{V}_A)^*}{J} G(A, D) e^{iqa}.
\end{aligned} \tag{A7}$$

Likewise, the last two equations yield

$$\begin{aligned}
G(B, B) \frac{V}{J} e^{iqa} - G(B, A) &= -G(B, D) \frac{(\bar{V}_A)^*}{J} e^{iqa}, \\
G(B, A) \frac{V}{J} e^{iqa} - G(B, B) &= \frac{1}{J} e^{iqa} - \frac{\bar{V}_B}{J} G(B, D) e^{iqa}.
\end{aligned} \tag{A8}$$

Hence, the solutions are

$$\begin{aligned}
G(A, D) &= -\frac{G(D, D)}{\frac{V^2}{J}e^{iqa} - Je^{-iqa}} \left(\bar{V}_A + \frac{V}{J}(\bar{V}_B)^* e^{iqa} \right), \\
G(B, D) &= -\frac{G(D, D)}{\frac{V^2}{J}e^{iqa} - Je^{-iqa}} \left((\bar{V}_B)^* + \frac{V}{J}\bar{V}_A e^{iqa} \right), \\
G(A, A) &= \frac{G(D, D)}{\frac{V^2}{J}e^{iqa} - Je^{-iqa}} \left(\epsilon_q - \epsilon_0 + \frac{V_B^2}{J} e^{iqa} \right), \\
G(B, B) &= \frac{G(D, D)}{\frac{V^2}{J}e^{iqa} - Je^{-iqa}} \left(\epsilon_q - \epsilon_0 + \frac{V_A^2}{J} e^{iqa} \right), \\
G(B, A) &= \frac{G(D, D)}{\frac{V^2}{J}e^{iqa} - Je^{-iqa}} \left(\frac{V}{J} e^{iqa} (\epsilon_q - \epsilon_0) - \frac{(\bar{V}_A \bar{V}_B)^*}{J} e^{iqa} \right), \\
G(A, B) &= \frac{G(D, D)}{\frac{V^2}{J}e^{iqa} - Je^{-iqa}} \left(\frac{V}{J} e^{iqa} (\epsilon_q - \epsilon_0) - \frac{\bar{V}_A \bar{V}_B}{J} e^{iqa} \right).
\end{aligned} \tag{A9}$$

Acknowledgements: We thank M. Heiblum, P. Wölfle, A. Schiller and D. Sprinzak for helpful conversations. O.E-W, A.A. and Y.I. thank the Institute for Theoretical Physics at the University of California, Santa Barbara

for its hospitality when this research was concluded and the paper written. This project was supported by the German-Israeli Foundation (GIF), by a Center of Excellence of the Israel Science Foundation, by the Albert Einstein Minerva Center for Theoretical Physics at the Weizmann Institute of Science and by the National Science Foundation under Grant No.PHY99-07949.

- [1] Y. Imry, *Introduction to Mesoscopic Physics* (Oxford University Press, Oxford 1997).
- [2] R. Landauer, *Philosoph. Mag.* **21**, 863 (1970).
- [3] Y. Aharonov and D. Bohm, *Phys. Rev.* **115**, 485 (1959).
- [4] Y. Gefen, Y. Imry and M. Ya. Azbel, *Phys. Rev. Lett.* **52**, 129 (1984).
- [5] R. A. Webb, S. Washburn, C. P. Umbach and R. B. Laibowitz, *Phys. Rev. Lett.* **54**, 2696 (1985).
- [6] T. K. Ng and P. A. Lee, *Phys. Rev. Lett.* **61**, 1768 (1988).
- [7] D. C. Langreth, *Phys. Rev.* **150**, 516 (1966).
- [8] L. Onsager, *Phys. Rev.* **38**, 2265 (1931).
- [9] O. Entin-Wohlman *et al.*, cond-mat/0108064 (unpublished).
- [10] e. g. R. P. Feynmann, R. B. Leighton and M. Sands, *The Feynmann Lectures on Physics*, Vol. III, Chap. 1 (Addison-Wesley, Reading 1970).
- [11] e. g. F. Schwabl, *Quantum Mechanics*, Sec. 7.5.2 (Springer-Verlag, Berlin, 1990).
- [12] A. Yacoby *et al.*, *Phys. Rev. Lett.* **66**, 1938 (1991).
- [13] A. Yacoby, M. Heiblum, V. Umansky, H. Shtrikman and D. Mahalu, *Phys. Rev. Lett.* **73**, 3149 (1994).
- [14] A. Yacoby, M. Heiblum, D. Mahalu and H. Shtrikman, *Phys. Rev. Lett.* **74**, 4047 (1994).
- [15] E. Buks *et al.*, *Phys. Rev. Lett.* **77**, 4664 (1996).
- [16] R. Schuster *et al.*, *Nature* **385**, 417 (1997).
- [17] Y. Ji, M. Heiblum, D. Sprinzak, D. Mahalu, and H. Shtrikman, *Science* **290**, 779 (2000).
- [18] Y. Ji, M. Heiblum and H. Shtrikman, cond-mat/0106469 (unpublished).
- [19] U. Gerland, J. von Delft, T. A. Costi and Y. Oreg, *Phys. Rev. Lett.* **84**, 3710 (2000).
- [20] U. Fano, *Phys. Rev.* **124**, 1866 (1961).
- [21] P.S. Deo and A.M. Jayannavar, *Mod. Phys. Lett.* **10**, 787 (1996); H. Xu and W. Sheng, *Phys. Rev. B* **57**, 11903 (1998); C.-M. Ryu and S. Y. Cho, *Phys. Rev. B* **58**, 3572 (1998); H.-W. Lee, *Phys. Rev. Lett.* **82**, 2358 (1999).
- [22] B. R. Bulka and P. Stefanski, *Phys. Rev. Lett.* **86**, 5128 (2001).
- [23] W. Hofstetter, J. König and H. Schoeller, cond-mat/0104497 (unpublished).
- [24] B. Shapiro, *Phys. Rev. Lett.* **50**, 747 (1983).
- [25] K. Kang and S.-C. Shin, *Phys. Rev. Lett.* **85**, 5619 (2000).
- [26] M. Büttiker, Y. Imry and M. Azbel, *Phys. Rev. A* **30**, 1982 (1984).
- [27] O. Entin-Wohlman, C. Hartzstein and Y. Imry, *Phys. Rev. B* **34**, 921 (1986).
- [28] J. König and Y. Gefen, *Phys. Rev. Lett.* **86**, 3855 (2001).
- [29] J. König, Y. Gefen and G. Schön, *Phys. Rev. Lett.* **81**, 4468 (1998).
- [30] G. Hackenbroich, W. D. Heiss and H. A. Weidenmüller, *Phys. Rev. Lett.* **79**, 127 (1997); R. Baltin *et al.*, *Eur. Phys. J. B.* **10**, 119 (1999); R. Baltin and Y. Gefen, *Phys. Rev. Lett.* **83**, 5094 (1999); G. Hackenbroich and R. A. Mendez, cond-mat/0002430 (unpublished).